

Montecarlo Application on Nucleon Dynamics in Calculating Fission Yield at 14 MeV Neutron Energy

Rizal Kurniadi¹

¹Nuclear Physics and Bio Physics Research Group, Institut Teknologi Bandung, INDONESIA

(Received: 20 June 2023, Revised: 30 July 2023, Accepted: 31 July 2023)

Abstract

Nuclear data is a completeness that must be present in every activity related to nuclear technology. So high is the role of nuclear data, it is necessary to have very complete nuclear data. The need for nuclear data is not in line with the resulting experimental products. The amount of experimental data needs to be completed. This is because the operational costs for these experiments are costly. Thus, theoretical modeling calculations are inevitably the right choice to replace experimental results. Many theoretical models have been developed to obtain satisfactory results. They were starting from microscopic models to macroscopic models. A common obstacle is that microscopic models must be simplified and efficient to produce massive nuclear data. Meanwhile, the constraints on the macroscopic model could be more accurate. This paper will present a calculation that tries to produce accurate but uncomplicated and economical data. This technique uses the basic principles of random numbers and classical nucleon dynamics in the nucleus. At the end of the paper, the results of calculations are presented, which are very accurate and, at the same time, show the dynamics of the nucleons that occur.

Keywords: Monte Carlo, Random Number, Fission Product Data, Macroscopic Framework.

INTRODUCTION

Experimental measurements of fission yield are minimal, which results in the ability to evaluate nuclear data is still limited[1]; 14 MeV energy is an important energy region for high energies, as described in [2][3]. At this energy, the behavior of fission products will begin to show, leading to an accumulation state around the symmetric product. Evaluating nuclear data for nuclear fission products (FPY) is very important to link nuclear fission experimental data, microscopic or macroscopic theory, or modeling with nuclear applications [4].

Considering that the nucleon system in the nucleus is a model of the many-body system, the multi-body quantum theory is a compelling microscopic approach to studying and predicting the state of the nucleons in a nucleus undergoing fission. Even though the quantum theory of many objects is compelling, the calculation technique is very complicated, requiring very high computational time. This method is in stark contrast to the practical requirements of nuclear data. For this reason, a theoretical method with lighter computation is

needed. A macroscopic model has been developed, which is a theoretical model that utilizes surface and coulomb energy simultaneously to generate deformation potentials. Through this deformation potential, the probability of fission formation will be generated. Even though the calculation and computation techniques are light, this macroscopic method cannot show the dynamics of the nucleons in the nucleus when the fission process occurs. Based on this fact, the mic-mac method has been developed [5-11]. Although the mi-mac method can increase detailed observation of macroscopic treatments, it still needs to be more economical.

Based on this, an idea about the nucleon dynamics model using random numbers was developed. Random numbers become the initiator of the beginning of the fission process. This random number initiates every fission event. The fission products are regulated through a nucleon dynamics mechanism that moves to form candidate nuclides. Through the random number bridge, the mic-mac method becomes more straightforward. Thus, this method proposes to calculate the fission yield through an economical technique that does not

¹* Corresponding author.

reduce the meaning of the nucleon dynamics process itself.

THE METHOD

This method begins by introducing the current density of movement of nucleons in the nucleus to be fissioned. The following equation expresses this current density,

we introduce three functions, namely "fitting function," "nuclide state function," and "nucleon state function." These three functions have nothing to do with the wave function, commonly known as the "quantum many-body problem." These three functions will be described in the following

$$J(A, \xi, \gamma) = \frac{\hbar}{2A_i} \int \left(\Psi^*(q: A, \xi, \gamma) \left(\frac{\partial}{\partial \xi} \Psi(q: A, \xi, \gamma) \right) - \Psi(q: A, \xi, \gamma) \left(\frac{\partial}{\partial \xi} \Psi^*(q: A, \xi, \gamma) \right) \right) dq \quad (1)$$

q is the coordinate of each nucleon. A is the mass number of the nuclide ξ is a parameter related to the shape of the nucleus and Ψ is wave function from slater determinant.

The fitting function is built by the state function of the two nuclides that will fission; this state function is composed of the state function of each nucleon incorporated into certain groups within the candidate nuclide. The formation of groups on candidate nuclides looks like a slatter determinant in GCM[12]. However, ξ in equation (1) is not a

paragraphs. The boundary condition for forming the "Fitting function" is the continuity equation. These boundary conditions ensure a continuous flow of nucleons from one fraction to another. Thus this fitting method will provide a classical picture of nucleon dynamics during the process.

This equation describes the nucleon dynamics affected by the shape of the deformed nucleus. According to the liquid drop model, changes in the shape of the nucleus's surface govern the movement of nucleons to form two new nucleon centers of mass together.

generator coordinate or any other collective coordinate [13-14]. The state function of the nucleon in this technique is obtained through the solution of the following equation,

$$-i \frac{\partial}{\partial \xi} \phi_{\tau, \nu, j}^k(q_\nu; A_\tau, \xi, t) = \mp \frac{1}{\sqrt{\pi\sigma_\nu}} \exp\left(-\frac{(\xi + \omega_{\nu, \tau} - (j-1)\Delta_{\nu, \tau} \pm \chi t)^2}{\sigma_\nu}\right) \phi_{\tau, \nu, j}^k(q_\nu; A_\tau, \xi, t) \quad (2)$$

k is the index for the fission mode, τ the index for the resulting nuclide, ν the group index, and j the index for the j -th nucleon.

$\omega_{\nu, \tau}$ indicates the width in the τ nuclide candidates, ν group. $\Delta_{\nu, \tau}$ is the distance between the two closest nucleons in the τ nuclide candidates ν group. At the same time, χ is related to the shifting scale each time the left and right nuclides leave the neck breakpoint.

Through this state function of the nucleon, the current density shown in equation (1) becomes,

$$J(A, \xi, t) = \mp \frac{\hbar}{A} \sum_{A_\tau} \sum_k \sum_\nu \sum_j \frac{\alpha_k^2 C_{A_\tau}}{\sqrt{\pi\sigma_\nu}} \exp\left(-\frac{(\xi + \omega_{\nu, \tau} - (j-1)\Delta_{\nu, \tau} \pm \chi t)^2}{\sigma_\nu}\right) \quad (2)$$

α and C are the expansion coefficients from the following equation,

$$\Psi = \sum_{A_\tau} C_{A_\tau} \psi_\tau \psi_{\tau-1} \quad (3)$$

$$\psi_\tau = \sum_k \alpha_k \Phi_{\tau,k} \quad (4)$$

$$\Phi_{\tau,k} = \prod_v \prod_j \phi_{\tau,v,j}^k \quad (5)$$

Equation (3) is an expression of the combination of possible state functions of the nuclide candidate ψ . In contrast, equation (4) of the state function of the candidate nuclide is a possible combination of the state functions of the fission mode Φ where the state function of this fission mode is constructed by the state function of each ϕ nucleon.

$$\rho(A, \xi, t) = \bar{\Gamma} q \frac{\hbar}{\chi A} \sum_{A_\tau} \sum_k \sum_v \sum_j \frac{\alpha_k^2 C_{A_\tau}}{\sqrt{\pi \sigma_v}} \exp \left(- \frac{(\xi + \omega_{v,\tau} - (j-1)\Delta_{v,\tau} \pm \chi t)^2}{\sigma_v} \right) \quad (7)$$

Based on the scission criteria in [15]: Limit to which a neck-breaking event occurs, the repulsive Coulomb force is considerable compared to the attractive force due to nuclear

interactions and due to the presence of surface energy, so the exchange force is neglected. Therefore, it can be concluded that there is no nucleon transfer between pre-fragmentation

nuclides. Thus it can be assumed that the density around the neck $\xi = 0$ will be constant. This condition results in the current density divergence being zero. Hence, it is reasonable

to assume that the current density is zero at the point $\xi = 0$.

Thus the resulting fission product is calculated through the following equation,

$$Y_\tau = A \int \rho(A, \xi, Y) d\xi \quad (8)$$

With,

$$\lim_{t \rightarrow Y} J(A, \xi = 0, t) = 0 \quad (8)$$

Y is the time when the current density equilibrium event is reached.

RESULTS AND DISCUSSION

Through the continuity equation obtained the probability density each time,

$$\rho(A, \xi, t) = \int \left(- \frac{\partial}{\partial \xi} J(A, \xi, t) \right) dt \quad (6)$$

explicitly the expression,

The fitting process is carried out through seven crucial data. These seven data are shown in the following figure,

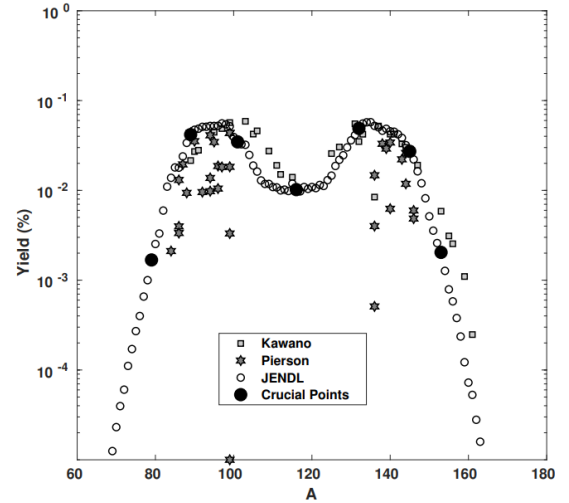


Fig. 2. The seven points that are included in the fitting process are represented by full black dots.

In Figure 1, the experimental results were obtained from Pierson[16] and Kawano[17]. Pierson's experimental results tend to approach standard fission mode 2 [18], while Kawano's experimental results are closely related to the data for high-yield values. In addition to these two experimental results, evaluation data from JENDL was also selected [19]. From the experimental and evaluation data, seven representative points were selected. These points are used as boundaries to calculate equation (8). The placement or selection of points follows the pattern

of fission mode [20] standard 1, standard 2, super long. Furthermore, the results of this fitting lead to equation (4), which is to perform a superposition of the various possible resulting fission modes. This addition refers to expanding a function of the probabilities that may occur.

To see the results of fitting these various fission modes shown in the following figure,

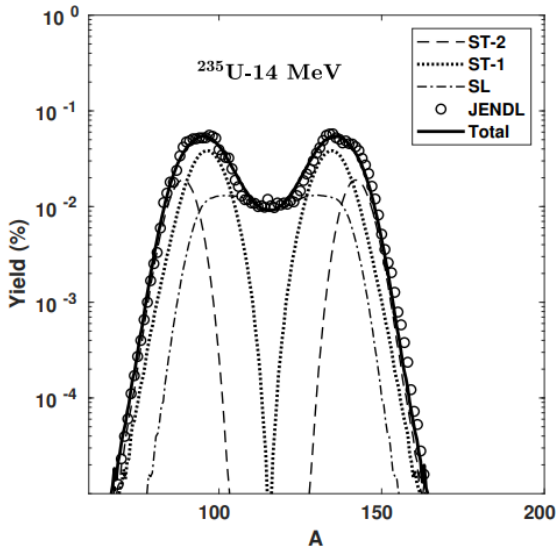
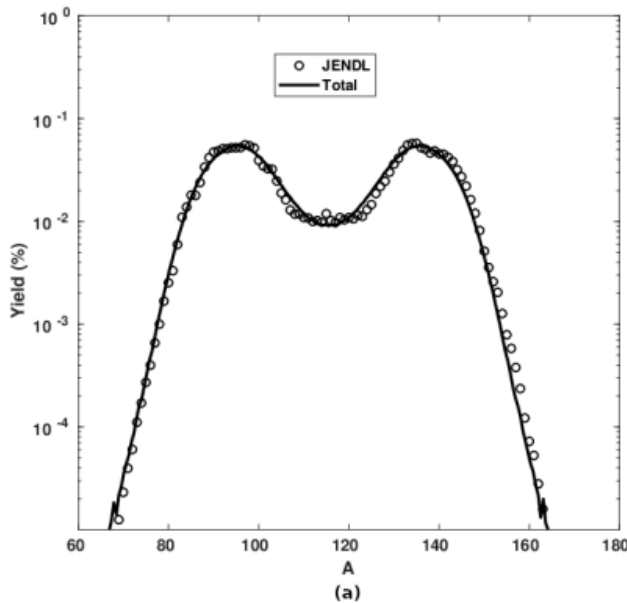


Fig. 3. Contribution of each mode to the formation of fission yield ^{235}U at the energy of 14 MeV.

This result is obtained through iteration of 10^6 times. The meaning of the number of iterations indicates that 10^6 fission events have occurred; from all of these

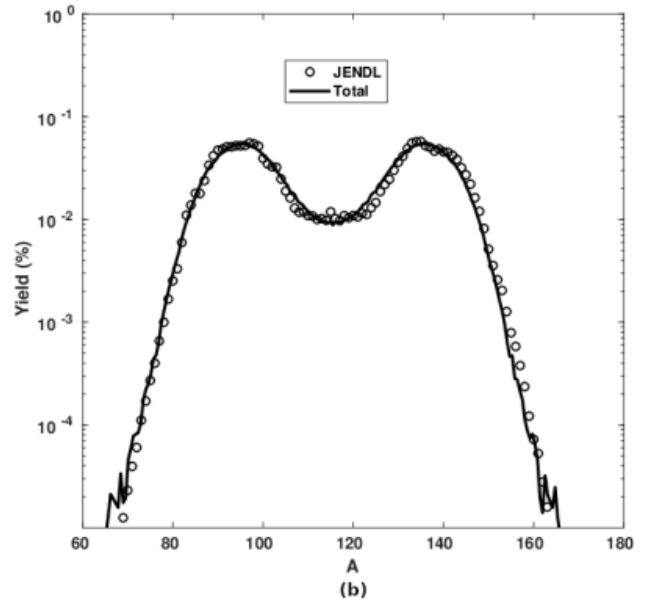


fission events, the general recapitulation is then carried out through the function expansion pattern as described in equations (3), (4), and (5).

The data calculated by this method is accurate enough to follow the JENDL-evaluated data pattern. Fission products demonstrate the role of the seven crucial points for the various fission modes involved. The symmetrical region almost follows the maximum fission yield value. The symmetrical region follows the results shown by Higgins experimentally [21]. Higgins showed that the greater the energy of the incoming neutrons, the higher the valleys would be. This result has been confirmed by previous work [22-24].

Referring to [25], the dash-dotted line is more similar to the super-long mode, while the others are similar to the standard 1 (dotted) and standard 2 (dashed). According to Brosa, super long is symmetrical fission with the most extended size. In contrast, standard is more towards antisymmetrical fission with a smaller distance than super long. Therefore, it is evident from Fig. 3 apart from super long, there are also standard 1 and standard 2 contributions, standard 2 for the asymmetric fission product curve, and standard 1 for the asymmetric and symmetrical fission product curve.

To see the effect of the number of iterations can be shown in the image below,



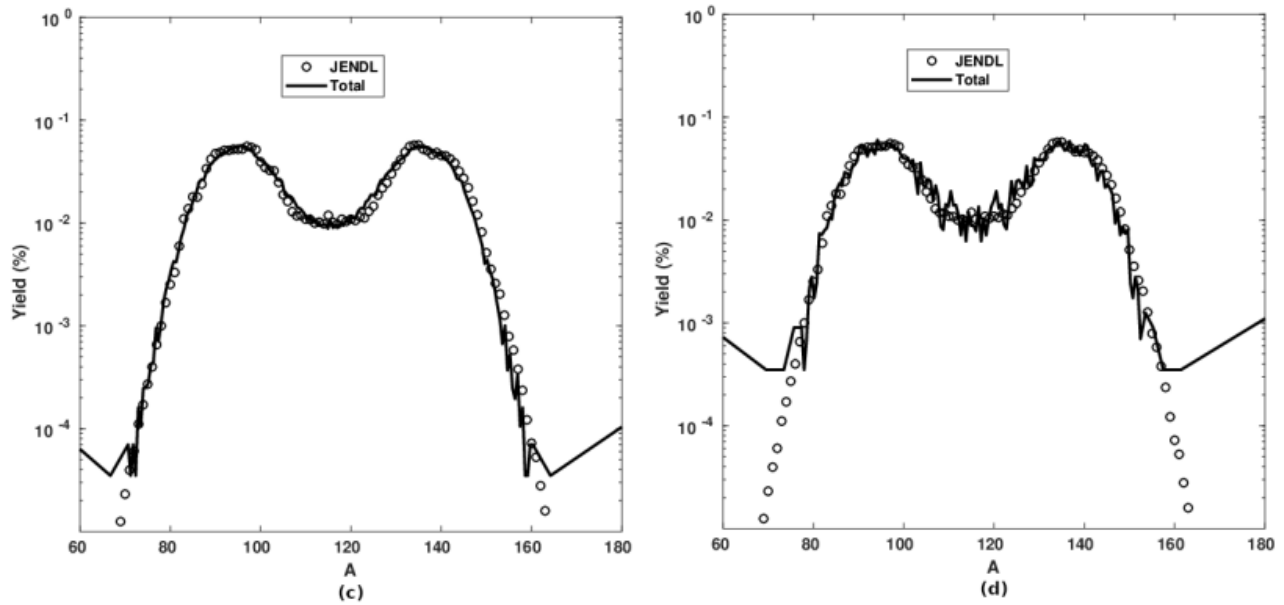


Fig. 4. Fission yield curves in a logarithmic scale for ^{235}U with a neutron energy of 14 MeV, (a) Fission events 10^6 times, (b) Fission events 10^5 times, (c) Fission events 10^4 times, (d) Fission events 10^3 times.

Through the picture, it is clear that the effect of the number of iterations on the results of the calculation of the fission yield is seen. The greater the

iteration, the smoother the curve will be. The results correspond to the basic concept of monte carlo.

CONCLUSION

Based on the results described in the previous section, this technique has demonstrated its accuracy in predicting fission yield data. In addition to its success in demonstrating accuracy, this technique has also demonstrated the nucleon dynamics that occur during the fission process. Fission yield calculations refer to the situation when nucleons are no longer transferred from the nuclide candidates. This condition is a solid basis of reference, bearing in mind that when the liquid drop model undergoes fission, there is no change in density between the nuclide candidates that will fission. The fission process is a directed random event, while the fission modes used as boundary conditions are the drivers.

Thus, using random numbers can be an alternative to calculating fission products without reducing the microscopic view of the nucleus. The nucleons are seen to follow their dynamics until an equilibrium point is reached.

ACKNOWLEDGMENT

Thanks are given to Prof. Anto Sulaksono for help and knowledge sharing.

REFERENCES

- (1) M. B. Chadwick et al., ENDF/B-VII.1 Nuclear Data for Science and Technology: Cross Sections, Covariances, Fission Product Yields and Decay Data, Nuclear Data Sheets 112, 2887 (2011) .
- (2) Z.-A. Wang and J. Pei, Optimizing multilayer Bayesian neural networks for evaluation of fission yields, Phys. Rev. C 104, 064608 (2021) .
- (3) M. Bender et al., Future of nuclear fission theory, J. Phys. G 47, 113002 (2020) .
- (4) L. A. Bernstein, D. A. Brown, A. J. Koning, B. T. Rearden, C. E. Romano, A. A. Sonzogni, A. S. Voyles, and W. Younes, Our Future Nuclear Data Needs, Ann. Rev.

- Nucl. Part. Sci 69, 109 (2019) .
- (5) N. Schunck and L. M. Robledo, Microscopic theory of nuclear fission: a review, *Rep. Prog. Phys* 79, 116301 (2016) ;
 - (6) K.-H. Schmidt and B. Jurado, Review on the progress in nuclear fission-experimental methods and theoretical descriptions, *Rep. Prog. Phys* 81, 106301 (2018) ;
 - (7) Y. Qiang, J. C. Pei, and P. D. Stevenson, Fission dynamics of compound nuclei: Pairing versus fluctuations, *Phys. Rev. C* 103, L031304 (2021) ;
 - (8) A. Bulgac, S. Jin, K. J. Roche, N. Schunck, and I. Stetcu, Fission dynamics of ^{240}Pu from saddle to scission and beyond, *Phys. Rev. C* 100, 034615 (2019) ;
 - (9) M. R. Mumpower, P. Jaffke, M. Verriere, and J. Randrup, Primary fission fragment mass yields across the chart of nuclides, *Phys. Rev. C* 101, 054607 (2020) ;
 - (10) L. L. Liu, X. Z. Wu, Y. J. Chen, C. W. Shen, Z. X. Li, and Z. G. Ge, impact of nuclear dissipation on the fission dynamics within the Langevin approach, *Phys. Rev. C* 105, 034614 (2022) ;
 - (11) J. Sadhukhan, S. A. Giuliani, Z. Matheson, and W. Nazarewicz, Efficient method for estimation of fission fragment yields of r-process nuclei, *Phys. Rev. C* 101, 065803 (2020)
 - (12) M. Rizea, N. Carjan, ANALYSIS OF THE SCISSION NEUTRONS BY A TIME-DEPENDENT APPROACH, *Proceedings of the Romanian Academy, Series A* 16, 176 (2015) .
 - (13) J. Zhao, T. Nikšić, D. Vretenar, and S-G. Zhou, Time-dependent generator coordinate method study of fission: Mass parameter, *Phys. Rev. C* 101, 064605 (2020) .
 - (14) M. Verriere and D. Regnier, The Time-Dependent Generator Coordinate Method in Nuclear Physics, *Frontier in Physics* 8, 233 (2020)
 - (15) W. Younes, D. Gogny, and J.-F. Berger, LLNL-BOOK-754886 (2018).
 - (16) B. D. Pierson, L. R. Greenwood, M. Flaska, S. A. Pozzi , Fission Product Yields from ^{232}Th , ^{238}U , and ^{235}U Using 14 MeV Neutrons, *Nuclear Data Sheets* 139, 171 (2017) .
 - (17) M. Mac Innes, M.B. Chadwick, T. Kawano, ENDF/B-VII.1 Nuclear Data for Science and Technology: Cross Sections, Covariances, Fission Product Yields and Decay Data, *Nuclear Data Sheets* 112, 2887 (2011) .
 - (18) P. Siegler, F.-J. Hamsch, S. Oberstedt, J.P. Theobald, Fission modes in the compound nucleus ^{238}Np , *Nucl. Phys. A* 594, 45 (1995) .
 - (19) J. Katakura, JENDL FP Decay Data File 2011 and Fission Yields Data File 2011, JAEAData/Code 2011-025, Japan Atomic Energy Agency, (2011)
 - (20) U. Brosa, S. Grossmann, A. Müller, and E. Becker, Nuclear scission, *Nucl. Phys. A* 502, 423 (1989) .
 - (21) Higgins et al., Fission fragment mass yields and total kinetic energy release in neutron-induced fission of ^{233}U from thermal energies to 40 MeV, *Phys. Rev. C* 101, 014601 (2020)
 - (22) V. Simutkin, Fragment Mass Distribution in Neutron-Induced Fission of ^{232}Th and ^{238}U from 10 to 60 MeV, Ph.D. thesis, Uppsala Universitet, 2010.
 - (23) V.D. Simutkin et al., Experimental Neutron-induced Fission Fragment Mass Yields of ^{232}Th and ^{238}U at Energies from 10 to 33 Me, *Nuclear Data Sheets* 119, 331 (2014) .
 - (24) T. R. England and B. F. Rider, ENDF-349: Evaluation and Compilation of Fission Product Yields (Tech. rep.), Los Alamos National Laboratory, (1994).
 - (25) U. Brosa, S. Grossmann, A. Müller, Nuclear Scission, *Phys. Rep.* 197, 4 (1990) . J. Lee, C. Gil, S. Hong, Calculation of fission product yields for uranium isotopes by using a semi-empirical model, *Eur. Phys. J. A* 54, 173, 2018.